Applied Thermal Engineering 29 (2009) 2921–2926

Contents lists available at ScienceDirect

Applied Thermal Engineering

journal homepage: www.elsevier.com/locate/apthermeng

Optimal design of a micro evaporator with lateral gaps

Taijong Sung [a], Daesik Oh [b], Sangrok Jin [a], Tae Won Seo [a,*], Jongwon Kim [a]

[a] Seoul National University, School of Mechanical and Aerospace Engineering, Seoul, Republic of Korea
[b] Core technology laboratory, Samsung SDI, Suwon, Republic of Korea

ARTICLE INFO

Article history:
Received 10 December 2008
Accepted 23 February 2009
Available online 1 March 2009

Keywords:
Micro evaporator
Optimal design
Design of experiment
Lateral gaps
Two-dimensional channel

ABSTRACT

This paper presents an optimal design of a micro evaporator, to maximize the heat transfer coefficient (HTC) and it forms the starting point in developing miniaturized vapor–compression refrigeration system. The experimental design is adopted to determine the optimal parameters of the evaporator for realizing the inlet–outlet conditions of the refrigerating cycle, and for increasing the HTC. The number of lateral gaps, channel width, and lateral gap size were optimized to maximize HTCs of 2062, 2029, and 1895 W/m^2K for heating powers of 40, 60, and 80 W, respectively. The refrigerant and the mass flow rate were fixed as R-123 and 0.72 g/s, respectively. Among the three design parameters, the channel width is the most sensitive parameter influencing the HTC. A periodic change of flow pattern was observed in the evaporator with high HTCs, and a dryout was observed in the evaporator with low HTCs.

1. Introduction

Recently, the heat dissipation of a mobile CPU has reached 95 W and cooling methods such as fan-fin and heat pipes have limitations because of the restricted space and the available heat transfer efficiency in laptop computers. Therefore, small-sized coolers based on vapor–compression refrigeration cycles, have been suggested as possible solutions [1–3]. Sung et al. [4] also proposed a stack-type active micro cooler having the size $50 \times 50 \times 15$ mm and having comparative advantages of space, cost, and being able to be mass produced.

The design of the evaporator is the starting point in developing effective active micro coolers because the inlet–outlet conditions of the evaporator have a standard design of expansion valve and compressor and so the heat transfer efficiency of the evaporator affects the performance of the whole system. The evaporation of the refrigerant in a micro channel has been widely researched, both theoretically and experimentally [5,6]. Lee and Lee [7] studied the correlation in order to represent the heat transfer coefficients of the boiling flow of R-113 through a rectangular channel of width of 20 mm and found that the heat transfer coefficient increased with the mass flux, and the local quality and the effect of heat flux appeared to be minor. They also found that the Kandlikar's flow boiling correlation covers the higher mass flux range, with a 10.7% mean deviation. Martin-Calizo et al. [8] experimentally investigated the subcooled flow boiling heat transfer, for R-134a, in vertical cylindrical tubes with various internal diameters of 0.83, 1.22, and 1.70 mm and found that the classical correlations of the boiling heat transfer could not predict the experimental heat transfer coefficient for all tested conditions.

To enhance the performance of the evaporator as a design standard for the active micro cooler, investigations of the phenomena inside the channel and optimizing the design of whole evaporator are clearly needed. However, the boiling phenomena inside the evaporator are difficult to define theoretically; even the theoretical setup cannot explain the phenomena in various conditions [8]. A few research studies have been carried out on the optimal design of the evaporator. Murata and Hijikata [9] analytically optimized the dimension of the cross-section of the evaporator; however, the experimental results were not demonstrated, Chiriac and Chiriac [10] compared the performance of the evaporator in a refrigeration system using R-134a for five cases; however, the optimization was not conducted in a systematic manner and only an ad-hoc trial-and-error method was adopted.

In this study, the design of experiment (DOE) methodology introduced by Taguchi [11] has been adopted for the optimal design of the evaporator; this is a good solution for optimizing the design of the evaporator, since the boiling phenomena inside the evaporator are difficult to define theoretically. It offers a simple and systematic approach to optimal design for the complicated system by using orthogonal arrays and signal to noise ratio. Details about the DOE are explained in the next section. Using the DOE methodology, the optimal design parameters were determined to

* Corresponding author. Address: Seoul National University, Mechanical Engineering, Shinlim 9-dong, Kwanak-gu, Bldg. 301, Rm. 210, Seoul 151-744, Republic of Korea. Tel.: +82 2 880 7144; fax: +82 2 875 4848.
E-mail addresses: taijsung@rodel.snu.ac.kr (T. Sung), daesik@rodel.snu.ac.kr (D. Oh), rokjin@rodel.snu.ac.kr (S. Jin), seotw@rodel.snu.ac.kr (T.W. Seo), jongkim@snu.ac.kr (J. Kim).

1359-4311/$ - see front matter © 2009 Elsevier Ltd. All rights reserved.
doi:10.1016/j.applthermaleng.2009.02.015

maximize the HTC based on the two-stage DOE and the two phase flow in the evaporator has also been visualized.

2. Design of experiment

2.1. Design of experiment methodology

The design of experiment methodology which is called Taguchi methodology is a robust optimal design methodology to find optimal values of design parameters which enable to maintain the best performance regardless of the external condition. The procedure of DOE is as follows [12];

(1) *Identifying the objectives:* In the first step of the DOE, identifying a specific objective is important. In this paper, the objective is an optimal design of the evaporator regardless to the heating power for maximizing the heat transfer coefficient.
(2) *Determining the quality characteristic:* The characteristic of quality is classified into 3 types; nominal-the-best, smaller-the-better, and larger-the-better. In this paper, the objective is maximizing the heat transfer coefficient, therefore it is a larger-the-better problem.
(3) *Selecting the controllable factors and noise factors:* The selection of factors to be tested for their influence on the quality characteristic is one of the most important procedure in DOE methodology. Careless selection of controllable factors and noise factors lead to false conclusion. After selecting the factors, their desired number of levels is determined. In this paper, the controllable factors are number of lateral gap, channel width, and lateral gap size and the noise factor is a heating power. All controllable factors are three levels to determine the optimal value.
(4) *Selecting an orthogonal array:* The exhaustive search of the optimal value requires the experiment of all combination of the factor levels under study. Orthogonal arrays provide smaller, less costly experiments. For example, a study involving 13 factors at three levels each would require 313 = 1,594,323 experiments with exhaustive search, while it would require only 27 experiments with $L_{27}(3^{13})$ orthogonal array.
(5) *Conducting the experiment and analysis:* The analysis of experiment relates to calculations for converting raw data into the representative signal-to-noise ratio (S/N ratio). By including the impact of noise factors on the process or product as the denominator, the S/N ratio can be adopted as the index of the system's ability to perform well regardless of the effects of noise. In this paper, optimal values of the factors to maximize the heat transfer coefficient in the evaporator regardless of the heating power was determined.

2.2. Experimental apparatus

As shown in Fig. 1, the experimental apparatus included in the optimization of the micro evaporator is comprised of the refrigerant transfer part, the test section, the camera, and the collecting container. The transfer part was composed of a gas pump with a pressure vessel, a flow meter, and a flow control valve. At the inlet and the outlet of the evaporator, pressure, and differential pressures transducers and two type-K thermocouples have been used to measure the pressure and temperatures of the refrigerant, respectively. A high speed camera (having a maximum frame rate of 10,000 fps) was used to observe the flow of the refrigerant inside the evaporator at 1000 fps as this gave sufficient resolution for the experiments performed.

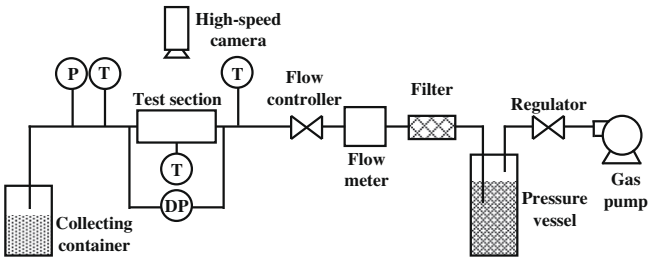

Fig. 1. Experimental apparatus.

The test section is shown schematically in Fig. 2 and is comprised of Pyrex glass, a micro evaporator chamber, and ceramic heater stacked between PEEK housings. A Teflon gasket and an O-ring seal were used to ensure a leak-proof contact between the Pyrex glass, the evaporator, and the ceramic heater. The thicknesses of the Pyrex glass, the evaporator, the ceramic heater, and the gasket were 1, 1.5, 1, and 2 mm, respectively. DC power supply which could be regulated in the ranges 0–30 V and 0–10 A was used to supply constant heat to the ceramic heater. The temperature of the heater was measured by a resistance temperature detector (RTD) which was attached at the bottom of the ceramic heater. The condition of the refrigerant at the inlet is shown in Table 1.

2.3. Data reduction

2.3.1. Pressure drop

The performance of the evaporator is evaluated by using the heat transfer coefficient and the pressure drop. Ideally, inside the evaporator, the pressure should be kept constant throughout the procedure; it was found that the pressure drop is not significant during the pre-tests and this can be seen in Fig. 3 which shows that the difference in pressure drop between the evaporators, for each heating power, is less than 0.02 bar. This is much lower than 1 bar, which is the pressure of the evaporator outlet. In this experiment, the pressure drop was therefore not used to determine optimal design parameters and so only the heat transfer coefficient was used for optimizing the design of the evaporator.

2.3.2. Heat transfer coefficient

As just stated the heat transfer coefficient was selected as the objective value for optimizing the design and the heat transfer coefficient of the evaporator is defined as follows:

$$h = \frac{Q_h}{A_s(T_w - T_r)} \tag{1}$$

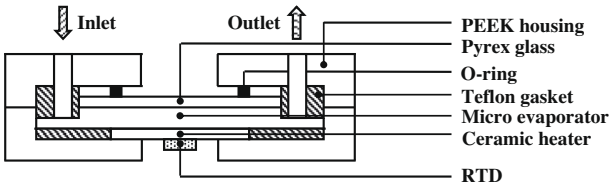

Fig. 2. Test section.

Table 1
Operating conditions of the experimental setup.

Refrigerant	Inlet temperature (°C)	Inlet pressure (bar)	Mass flow rate (g/s)	Power of heater (W)
R-123	25	1.0	0.72	40, 60, 80

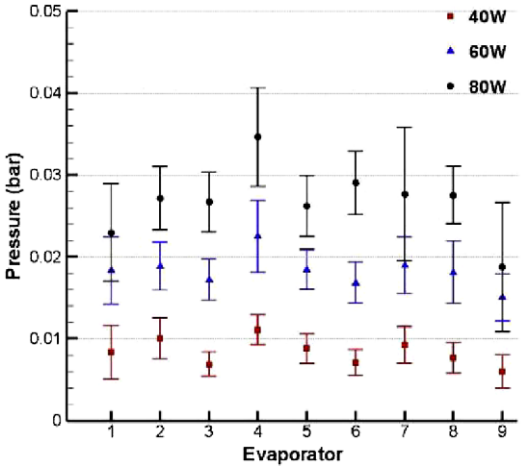

Fig. 3. Pressure drop in the micro evaporators.

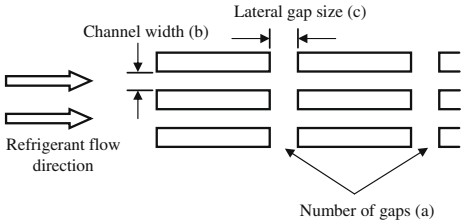

Fig. 4. Definition of the design parameters.

Table 2
Design parameters at the various levels.

	Level 1	Level 2	Level 3
a (Number of gaps)	2	3	4
b (Channel width)	0.2 mm	0.35 mm	0.5 mm
c (Lateral gap size)	0.5 mm	0.75 mm	1.0 mm

where Q_h is the heating power of the heater which is given as 40 W, 60 W, and 80 W, respectively, A_s is a surface area inside the evaporator, T_w and T_r are temperatures of the wall and the refrigerant, respectively. However, as it is not possible to measure these T_w and T_r directly in the experiment the heat transfer coefficient has been calculated based on the relation from the values that can be measured from the experiment.

T_w can be calculated by using the one-dimensional heat transfer equation from the heater to the evaporator:

$$T_w = T_h - \frac{q_h t}{k_{al}} \tag{2}$$

where q_h is a heat flux from heater which is 1.48 W/m^2 for the heating power of 80 W, and T_h is the temperature of the heater, t is thickness of the evaporator, which is 0.5 mm, and k_{al} is the conductivity of aluminum, which is 237 W/m K. By inserting the parameter values $T_h - T_w = 0.312$ °C is obtained, so it can be assumed that T_w and T_h are approximately the same value.

Since the refrigerant is supplied in a sub-cooled state, the evaporator can be divided into two regions: an upstream sub-cooled region and a downstream saturated region. The area that the sub-cooled refrigerant occupies can be calculated by the energy balance equation:

$$\frac{A_l}{A_s} = \frac{\dot{M}C(T_{sat} - T_{in})}{Q_h} \tag{3}$$

where A_l is the area of saturated liquid inside the evaporator, $\dot{M}$ is the mass flow rate of refrigerant, which is 0.72 g/s, C is specific heat of the refrigerant, which is 0.965 kJ/kg K for the liquid state. And T_{sat} is the saturation temperature of the refrigerant, which is 27.85 °C for 1.013 bar, T_{in} is the temperature of the refrigerant at the inlet, which is 25 °C. By inserting the parameter values, the ratio of the sub-cooled area to the total area was obtained as 4.95×10^{-2} for the heating power of 40 W, which means that the saturated vapor occupies more than 95% of the total area of the evaporator for the worst case. Therefore it can be assumed that the temperature of the refrigerant is the same as the temperature of the saturated gas ($T_w \approx T_{sat}$).

Then the relation between the objective value and the measured values is determined by using:

$$h' = \frac{Q_h}{A_s(T_h - T_{sat})} \tag{4}$$

The objective of this research is to find the optimal parameter set, to maximize h', which is a modified heat transfer coefficient.

2.4. Design parameters and constraints of the experimental studies

Three parameters were selected to be optimized, namely the number of gaps, the channel width, and the lateral gap size. The lateral gap was introduced to reduce the flow instability by dispersing the vapor bubbles to the lateral direction. A graphical explanation of each parameter is shown in Fig. 4. From practical constraints, the height of the fin was fixed as 1 mm and the width, the length, and the height of the evaporator were fixed as 50 mm, 50 mm, and 1.5 mm, respectively.

The candidates for the design parameters are shown in Table 2. To select the best parameter set, nine experiments were conducted using the $L_9(3^4)$ orthogonal array [11]. The power of the heater is selected as a noise factor and the orthogonal array is presented in the left side of Table 3. Along the $L_9(3^4)$ orthogonal array, nine evaporators, made of aluminum, were manufactured as shown in Fig. 5.

3. Optimal design by experimental investigations

3.1. Intermediate result of optimal design

Along the $L_9(3^4)$ array, shown in the left side of Table 3, nine sets of experiments were conducted and the temperature of the heater was measured in each case. The experimental result is shown in the right side of Table 3 and its error analysis is shown in Fig. 6. As shown in the Fig. 6, there is little error on the investigated data. Eq. (4) and the parameter values mentioned above have been used to calculate the heat transfer coefficient and the S/N ratio (signal-to-noise ratio) was also calculated to analyze the sensitivity of the parameters regardless of noise factor. Since the heat transfer coefficient was expected to be high at the optimized evaporator, a larger-the-better S/N ratio was selected where the larger-the-better S/N ratio is defined as follows:

$$S/N = -10\log\frac{|\sum_{i=1}^{n} 1/y_i^2|}{n} \tag{5}$$

where y_i is the measured output and n is the number of experiments.

By performing the sensitivity analysis shown in Fig. 7, the intermediate optimal parameter set for the three gaps considered, led to the channel width of 0.5 mm and lateral gap size of 0.5 mm being identified as the best with a corresponding S/N ratio of 57.80 dB, 60.34 dB, and 58.77 dB, respectively. Among the three parameters, the channel width was determined to be the most sensitive parameter to the heat transfer coefficient. Although the best parameter

Table 3
Intermediate experimental results based on orthogonal array $L_9(3^4)$ in the design of experiment.

Experiment number	Design parameters			T_h (°C)			h (W/m^{2}K)			*S*/*N* ratio (dB)
	a	b (mm)	c (mm)	40 W	60 W	80 W	40 W	60 W	80 W	
1-1	2	0.2	0.5	50.21	90.95	138.5	790.3	420.1	319.5	52.45
1-2	2	0.35	0.75	41.92	58.99	107.2	1472	997.7	522.4	57.67
1-3	2	0.5	1.0	41.88	52.47	83.15	1657	1416	840.8	61.20
1-4	3	0.2	0.75	64.48	102.8	138.5	493.9	362.3	327.1	51.54
1-5	3	0.35	1.0	42.66	58.00	113.8	1440	1061	496.0	57.42
1-6	3	0.5	0.5	39.16	46.10	60.09	1973	1834	1384	64.45
1-7	4	0.2	1.0	53.42	91.42	134.9	714.3	431.0	341.3	52.75
1-8	4	0.35	0.5	40.47	54.41	86.19	1556	1109	673.0	59.41
1-9	4	0.5	0.75	49.57	71.69	138.0	1029	764.9	406.1	55.37

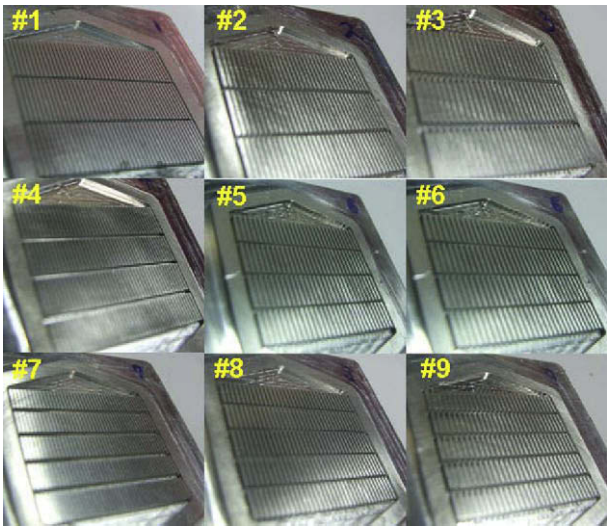

Fig. 5. Pictures of the micro evaporators constructed for the experimental studies.

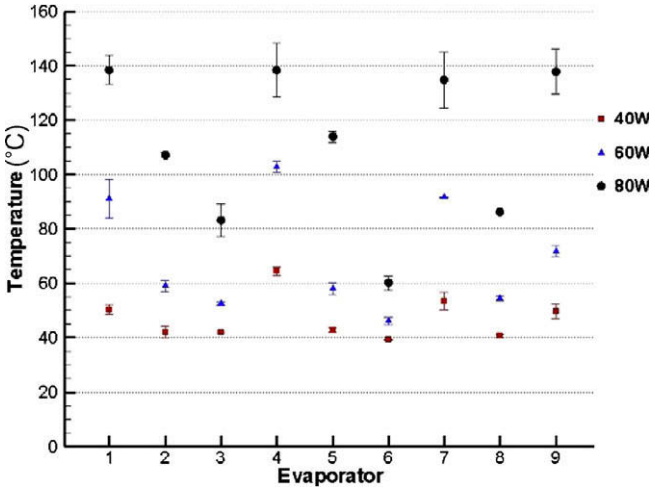

Fig. 6. Measured temperatures and their error analysis.

set corresponded with the 6th evaporator, further experiments should be conducted to obtain the optimal evaporator overall.

3.2. Final results of the optimal design

Based on the intermediate result, the second stage of experiments was designed where the channel width and the lateral gap size were modified. Because the tendency of the lateral gap size showed a bi-directional increase with a minimum at a gap size of 0.75 mm, two sets of $L_4(2^3)$ orthogonal array were used, as shown in the left side of Table 4.

The final result of the optimal design is shown in the right side of Table 4. The sensitivity analysis can be conducted again with the *S*/*N* ratio for the second stage but the final optimal *S*/*N* ratio, and the intermediate optimal *S*/*N* ratio have a difference of 1.53 dB, and the deviation of the second stage of experiment is 4.78 dB, which is much lower than the value at the first stage of the experiment, namely, 12.92 dB. This means that the heat transfer coefficient has almost reached the maximum at the second experimental stage, and the sensitivity analysis here is meaningless. Therefore, it can be decided that the result of the second stage experiments yields the optimal parameter set to maximize the heat transfer coefficient. Assuming this, the optimized evaporator can be concluded with the combination of variables having smallest *S*/*N* ratio, as presented in Table 4, which are three gaps, channel width of 0.65 mm, and lateral gap size of 1.25 mm.

4. Flow visualization

During the experiments performed to obtain the optimal design of the evaporator, observations of the flow of refrigerant inside the evaporator were conducted by using a high speed camera, located above the test section, for 0.5 s at 1000 fps. Through the flow visualization, it was seen that the flow pattern of the refrigerant depended on the power of the heater and the values of the design parameters.

The observed flow inside 6th prototype of the micro evaporator at 40 W is analyzed sequentially in time as shown in Fig. 8. An elongated vapor slug of refrigerant occupies the channel and the lateral gap (see Fig. 8a). The liquid refrigerant flushes into the channel and fills the channel (see Fig. 8b). The wall-nucleating bubbles are generated at the channel wall (see Fig. 8c). The bubbles are confined by the channel wall and coalesce with other bubbles to form a vapor slug (see Fig. 8d). The vapor slugs merge together and become an elongated vapor slug (see Fig. 8e) and the process is repeated. This periodic change is caused by a local increase of pressure drop across the channel and as the vapor slug grows, the pressure drop at that position increases. When the pressure drop reaches a threshold value, the vapor slug is swept away by the liquid refrigerant.

Fig. 9 shows photographs of the refrigerant flow of the 6th prototype of the micro evaporator at 80 W where the periodic change of flow regime also occurs, however, it is different from that at 40 W in the following aspects. The photograph is a flow regime before the liquid refrigerant flushes into the channel. The flow regime is an annular flow although it seems to be the elongated vapor slug, as shown in Fig. 9a. If it is an elongated vapor slug, it will move to the outlet when the liquid flushes into the channel but the vapor does not move and the liquid flow along the liquid film at the wall

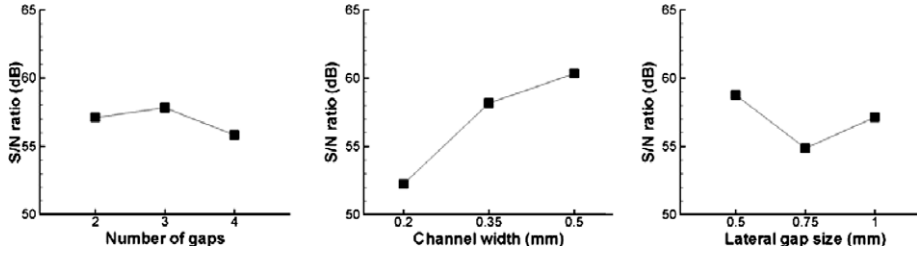

Fig. 7. Sensitivity analysis for each design parameter.

Table 4
Final experimental results based on two tries of orthogonal array $L_4(2^3)$ in the design of experiment.

Experiment number	Design parameters			T_h (°C)			h (W/m^{2}K)			*S*/*N* ratio (dB)
	a	b (mm)	c (mm)	40 W	60 W	80 W	40 W	60 W	80 W	
2-1	3	0.5	1.0	41.88	52.47	83.15	1657	1416	840.8	61.20
2-2	3	0.5	1.25	39.93	46.05	53.78	1916	1908	1785	65.42
2-3	3	0.65	1.0	40.43	46.87	55.86	1944	1929	1746	65.42
2-4	3	0.65	1.25	39.99	46.35	54.27	2062	2029	1895	65.98
2-5	3	0.5	0.25	43.73	52.98	62.94	1324	1255	1199	61.98
2-6	3	0.5	0.5	39.16	46.10	60.09	1973	1834	1384	64.45
2-7	3	0.65	0.25	40.42	47.78	59.02	1820	1722	1468	64.35
2-8	3	0.65	0.5	40.21	46.59	54.40	1892	1872	1761	65.29

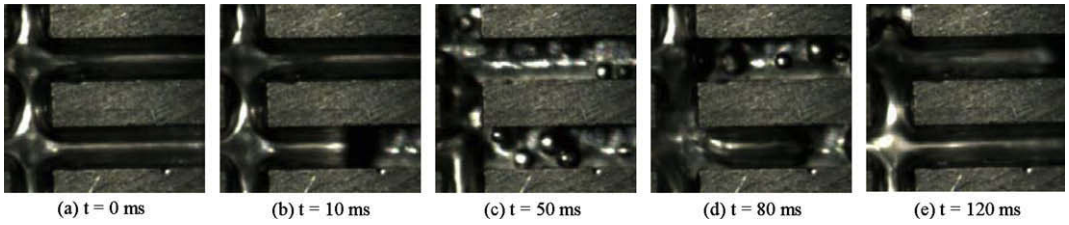

Fig. 8. Periodic change of flow pattern in the 6th evaporator at 40 W.

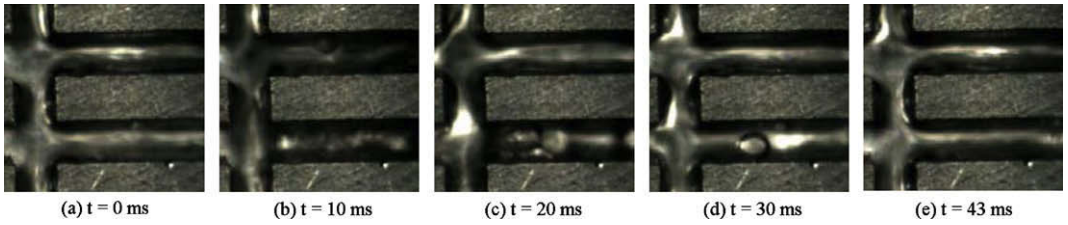

Fig. 9. Flow pattern of the 6th evaporator at 80 W.

of the evaporator (see Fig. 9b and c). As shown in Fig. 9d, the nucleation occurs in the thin liquid film on the channel wall. The period of the change reduces from 120 ms to 43 ms.

Fig. 10a and b show the photographs of the refrigerant flow of the 4th prototype of the micro evaporator at 40 W and 80 W, respectively, where it can be seen that the periodic change of flow regime is not observed. At 40 W, the liquid film of refrigerant is formed on the wall of the channel and the gap so that the nucleation on the wall occurs only in the gap side of the channel (see Fig. 10a). At 80 W, the dryout of the refrigerant occurred inside the evaporator, so the flow of refrigerant is not observed (see Fig. 10b).

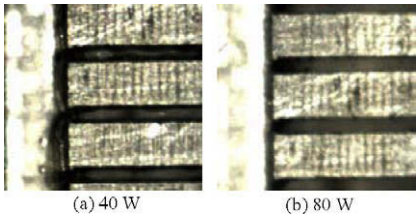

Fig. 10. Flow patterns of the 4th evaporator at 40 W and 80 W.

5. Conclusion

In this paper, the optimal parameters have been designed to maximize the heat transfer coefficient. The selected parameters are the number of gaps, the channel width, and the lateral gap size and the optimal parameter set bas been determined as 3, 0.65 mm and 1.25 mm, respectively. The maximized heat transfer coefficients are 2062, 2029, and 1895 W/m^{2}K for the heater powers of 40, 60, and 80 W, respectively. From the sensitivity analysis, the channel width is the most sensitive parameter amongst the design parameters. By the flow observation during the intermediate

experiments, it was found that the periodic change of flow pattern occurs at the evaporator with a high heat transfer coefficient, while the dryout occurs at the evaporator with a low heat transfer coefficient. To develop an active micro-cooler, the development of a miniaturized expansion valve and a condenser is processing and further studies are planned.

Acknowledgements

This work is sponsored by the Brain Korea 21 program and Engineering Research Center for Micro-thermal Systems.

References

[1] A.G. Agwu Nnanna, Application of refrigeration system in electronics cooling, Applied Thermal Engineering 26 (1) (2006) 18–27.
[2] P.E. Phelan, J. Swanson, Designing a mesoscale vapor–compression refrigerator for cooling high-power microelectronics, in: 9th Inter Society Conference on Thermal Phenomena, 2004, pp. 218–223.
[3] S. Trutassanawin, E.A. Groll, S.V. Garimella, L. Cremaschi, Experimental investigation of a miniature-scale refrigeration system for electronics cooling, IEEE Transaction on Component and Packaging Technologies 29 (3) (2006) 678–687.
[4] T. Sung, D. Oh, T. Seo, J. Kim, Optimal design of a micro evaporator to maximize heat transfer coefficient, Asian Symposium for Precision Engineering and Nanotechnology (2007) 63–66.
[5] B. Agostini, B. Watel, A. Bontemps, B. Thonon, Friction factor and heat transfer coefficient of R134a liquid flow in mini-channels, Applied Thermal Engineering 22 (16) (2002) 1821–1834.
[6] X. Huo, L. Chen, Y.S. Tian, T.G. Karayiannis, Flow boiling and flow regimes in small diameter tubes, Applied Thermal Engineering 24 (8-9) (2004) 1225–1239.
[7] H.J. Lee, S.Y. Lee, Heat transfer correlation for boiling flow in small rectangular horizontal channels with low aspect ratios, International Journal of Multiphase Flow 27 (2001) 2043–2062.
[8] C. Martin-Calizo, B. Palm, W. Owhaib, Subcooled flow boiling of R-134a in vertical channels of small diameter, International Journal of Multiphase Flow 33 (2007) 822–832.
[9] K. Murata, K. Hijikata, Optimization of a two-phase flow evaporator by varying the channel cross-section, Heat Transfer – Japanese Research 26 (3) (1997) 143–158.
[10] V. Chiriac, F. Chiriac, The optimization of refrigeration vapor compression system for power microelectronics, in: 10th Intersociety Conference on Thermal Phenomena, 2006, pp. 759–764.
[11] G. Taguchi, Taguchi on Robust Technology Development: Bringing Quality Engineering Upstream, ASME Press, 1993.
[12] K. Lee, J. Kim, Controller gain tuning of a simultaneous multi-axis PID control system using the Taguchi method, Control Engineering Practice (8) (2000) 949–958.